

Synthesis and Structure of $\text{LaSc}_2\text{N}@C_s(\text{hept})\text{-C}_{80}$ with One Heptagon and Thirteen Pentagons**

Yang Zhang, Kamran B. Ghiassi, Qingming Deng, Nataliya A. Samoylova, Marilyn M. Olmstead,* Alan L. Balch,* and Alexey A. Popov*

Abstract: The synthesis and single-crystal X-ray structural characterization of the first endohedral metallofullerene to contain a heptagon in the carbon cage are reported. The carbon framework surrounding the planar LaSc_2N unit in $\text{LaSc}_2\text{N}@C_s(\text{hept})\text{-C}_{80}$ consists of one heptagon, 13 pentagons, and 28 hexagons. This cage is related to the most abundant $I_h\text{-C}_{80}$ isomer by one Stone–Wales-like, heptagon/pentagon to hexagon/hexagon realignment. DFT computations predict that $\text{LaSc}_2\text{N}@C_s(\text{hept})\text{-C}_{80}$ is more stable than $\text{LaSc}_2\text{N}@D_{5h}\text{-C}_{80}$, and suggests that the low yield of the heptagon-containing endohedral fullerene may be caused by kinetic factors.

According to the IUPAC definition, fullerenes are “Compounds composed solely of an even number of carbon atoms, which form a cage-like fused-ring polycyclic system with twelve five-membered rings and the rest six-membered rings”, although the broadened definition also includes any closed cage structures consisting of three-coordinate carbon atoms.^[1] The number of pentagons in this definition follows from Euler’s theorem as applied to a polyhedron comprising only pentagons and hexagons. Furthermore, it was found that adjacent pentagons are strongly destabilizing, and hence the isolated pentagon rule (IPR) was formulated.^[2] The IPR requires that each pentagon be surrounded by five hexagons and is rooted in the anti-aromaticity of the pentalene fragment and its high curvature, thus leading to the significant strain in an sp^2 -based carbon system.

Fullerenes with polygons other than hexagons and pentagons have been studied theoretically.^[3] The structural

consequences from Euler’s theorem applied to fullerenes with pentagons, hexagons, and heptagons are discussed in detail by Fowler et al.^[3c] For such a polyhedron, the difference between the number of pentagonal and heptagonal faces is twelve. Therefore, addition of a heptagon increases the number of pentagons by one, while decreasing the number of hexagons by two. Fowler et al. also showed that, in contrast to strongly destabilizing pentagon/pentagon edges, the pentagon/heptagon edges are energetically favorable and their number should be maximized.^[3c] As a result, the most stable isomers of heptagon-containing fullerenes usually involve a heptagon fused to an adjacent pentagon pair.

The heptagon-containing fullerenes are usually less stable than IPR cages, and their formation in a standard arc-discharge synthesis has never been observed. However, if the fullerene π system is modified and some cage atoms are sp^3 hybridized, the stability factors such as the IPR are no longer applicable. Exohedral derivatization can stabilize the “defects” (e.g., pentagon adjacencies),^[4] which makes heptagon-containing fullerenes possible. Among the seven reported fullerene structures with heptagonal faces, six were obtained by “etching” the fullerene surface with fluorine or chlorine under relatively harsh reaction conditions,^[5] and one was synthesized by introduction of CCl_4 to the carbon arc.^[6] In all of these structures except for one (which has no adjacent pentagons),^[5c] the pentagon adjacencies accompanying the heptagon ring are stabilized by exohedral addition of halogen atoms, thus consequently transforming the halogenated carbon atoms from sp^2 to sp^3 . Metal ions encapsulated inside the fullerene cage can also stabilize pentagon adjacencies.^[4,7] In fact, the number of structurally characterized non-IPR endohedral metallofullerenes (EMFs) is comparable to that of ones obeying the IPR. Thus, the IPR is only a suggestion, not a rule, for endohedral fullerenes.^[7d,e]

Herein we demonstrate that endohedral metallofullerenes with heptagonal rings can be obtained in the arc-discharge synthesis and characterize the first EMF with a heptagon, $\text{LaSc}_2\text{N}@C_s(\text{hept})\text{-C}_{80}$, by single-crystal X-ray diffraction. Second, our computational study reveals that an EMF with heptagonal rings can be as stable as conventional EMFs, and the fact that they have not been discovered before is due to their low yields, and not to their thermodynamic stability.

Three isomers of $\text{LaSc}_2\text{N}@C_{80}$, $\text{LaSc}_2\text{N}@I_h\text{-C}_{80}$, $\text{LaSc}_2\text{N}@D_{5h}\text{-C}_{80}$, and the heptagon-containing C_s -symmetric $\text{LaSc}_2\text{N}@C_s(\text{hept})\text{-C}_{80}$, were synthesized along with the other mixed-metal La-Sc nitride clusterfullerenes in the arc-discharge synthesis and isolated from the fullerene mixture using high-pressure liquid chromatography (see the Supporting Information for further details). Figure 1 shows the molecular

[*] Dr. Y. Zhang, Q. Deng, N. A. Samoylova, Dr. A. A. Popov
Leibniz Institute for Solid State and Materials Research
Helmholtzstrasse 20, 01069 Dresden (Germany)
E-mail: a.popov@ifw-dresden.de

K. B. Ghiassi, Prof. M. M. Olmstead, Prof. A. L. Balch
Department of Chemistry, University of California
Davis, CA 95616 (USA)
E-mail: mmolmstead@ucdavis.edu
albalch@ucdavis.edu

[**] Financial support from the DFG (grant PO 1602/1-1 to A.A.P.) and the U.S. NSF (Grant CHE-1305125 to A.L.B. and M.M.O.) is gratefully acknowledged. We thank the Advanced Light Source, supported by the Director, Office of Science, Office of Basic Energy Sciences, of the U.S. Department of Energy under Contract No. DE-AC02-05CH11231, for beam time, and Dr. Simon J. Teat for his assistance. Computational resources were provided by the Supercomputing Center of Moscow State University and Center for Information Services and High Performance Computing (ZIH) in TU Dresden.

Supporting information for this article is available on the WWW under <http://dx.doi.org/10.1002/ange.201409094>.

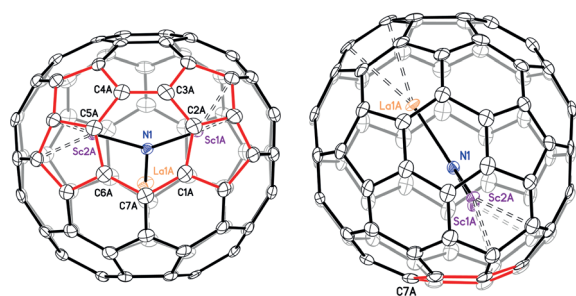


Figure 1. Two views of the structure of $\text{LaSc}_2\text{N}@C_s(\text{hept})\text{-C}_{80}$ as determined by a single-crystal X-ray diffraction study of the cocrystal, $\text{LaSc}_2\text{N}@C_s(\text{hept})\text{-C}_{80} \cdot 2 \text{Ni}(\text{OEP}) \cdot 2 \text{toluene}$, drawn with 30% thermal contours. The position of the heptagon and the two adjacent pentalene units is highlighted in red in the structure pictured on the left, while only the heptagon, which is nonplanar, is colored red in the structure pictured on the right. The dashed lines show the contacts between the metal ion and the nearest cage carbon atoms. The second orientation of the cage, the toluene molecules, and the hydrogen atoms were omitted for clarity.

structure of $\text{LaSc}_2\text{N}@C_s(\text{hept})\text{-C}_{80}$ from a cocrystal grown with $\text{Ni}(\text{OEP})$ (OEP = octaethylporphyrin). In agreement with Euler's theorem, C_{80} with one heptagonal face has 13 pentagons and 28 hexagons. The heptagon and the two flanking pentalene units are highlighted in red. As usually observed, metal ions, in this case the Sc ions, are located near the pentalene units. The LaSc_2N unit inside the cage is flat, but the heptagon is not. As seen at the bottom of the figure, the heptagon is folded along the line between C5A and C2A. The dihedral angle between the relatively planar C5A, C6A, C7A, C1A, and C2A portion and the planar C5A, C4A, C3A, and C2A portion is $158.05(7)^\circ$. In contrast, hexagons and pentagons in fullerenes are usually planar as they are here in $\text{LaSc}_2\text{N}@C_s(\text{hept})\text{-C}_{80}$. In other aspects, the structure of $\text{LaSc}_2\text{N}@C_s(\text{hept})\text{-C}_{80}$ resembles that of its isomer, $\text{LaSc}_2\text{N}@I_h\text{-C}_{80}$, which was described earlier.^[8] There is disorder in the crystal structure of $\text{LaSc}_2\text{N}@C_s(\text{hept})\text{-C}_{80}$ as described in the Supporting Information.

To reveal the influence of the heptagonal face and non-uniform distribution of pentagons in $\text{LaSc}_2\text{N}@C_s(\text{hept})\text{-C}_{80}$ on its stability, we have performed a series of DFT computations. The synthesis of nitride clusterfullerenes usually yields two isomers with the C_{80} cage and is dominant in the $\text{M}_3\text{N}@C_{2n}$ fullerene mixture.^[9] The most abundant isomer has I_h -cage symmetry, whereas the second most abundant structure is the isomer with the D_{5h} cage. Both isomers have enhanced stability because of the uniform distribution of pentagons minimizing the on-site Coulomb repulsion of six electrons transferred to the fullerene from the endohedral cluster.^[10] Table 1 lists relative energies of C_{80}^{6-} and nitride clusterfullerenes with different clusters encapsulated within the three isomers of C_{80} . For all studied compounds, the isomers with the I_h C_{80} cage have the lowest energies, and are therefore used as a reference. In the empty, hexaanionic state, $C_s(\text{hept})\text{-C}_{80}$ is 171 kJ mol^{-1} less stable than the I_h isomer. The D_{5h} isomer is the second most stable with the relative energy of 88 kJ mol^{-1} . Note that with such a high relative energy, $C_s(\text{hept})\text{-C}_{80}$ is still the third most stable isomer of C_{80}^{6-} (see

Table 1: Relative energies (kJ mol^{-1}) of three C_{80}^{6-} and $\text{M}_3\text{N}@C_{80}$ cage isomers.^[a]

	I_h	D_{5h}	$C_s(\text{hept})$
C_{80}^{6-}	0	88	171
$\text{LaSc}_2\text{N}@C_{80}$	0	61	27
$\text{Y}_3\text{N}@C_{80}$	0	70	31
$\text{Sc}_3\text{N}@C_{80}$	0	67	92

[a] DFT calculations are performed at the PBE/TZ2P level with SBK-type effective core potential basis set for Sc, Y, and La atoms as implemented in Priroda package.^[11]

Ref. [10a] and Table S2 in the Supporting Information for relative energies of other isomers). Encapsulation of nitride clusters only slightly affects the relative stability of the D_{5h} isomers (it varies in the $60\text{--}70 \text{ kJ mol}^{-1}$ range depending on the cluster), but stability of the $C_s(\text{hept})\text{-C}_{80}$ isomer is dramatically enhanced. $\text{LaSc}_2\text{N}@C_s(\text{hept})\text{-C}_{80}$ is only 27 kJ mol^{-1} less stable than the I_h isomer and is therefore substantially more stable than the D_{5h} isomer (note that the configuration of the LaSc_2N cluster with an La atom coordinating one of the pentalene unit is 49 kJ mol^{-1} less stable than the experimentally observed structure). A similarly high stability is predicted for the $\text{Y}_3\text{N}@C_s(\text{hept})\text{-C}_{80}$ (31 kJ mol^{-1}). Only for the smaller Sc_3N cluster is the relative energy of $\text{Sc}_3\text{N}@C_s(\text{hept})\text{-C}_{80}$ higher than that of the $\text{Sc}_3\text{N}@D_{5h}\text{-C}_{80}$ isomer. To ensure that these values are not the result of an artifact of a given density functional and basis set (PBE/TZ2P), we performed a series of calculations using different functionals and found similar results (see the Supporting Information).

Thus, the DFT study revealed an unexpectedly high stability for the $\text{M}_3\text{N}@C_s(\text{hept})\text{-C}_{80}$ isomer. For nitride clusters with large metals (Y and presumably lanthanides, which have similar ionic radii) the heptagon-containing isomer is considerably more stable than the D_{5h} cage. If the isomeric distribution would be governed by the thermodynamic stability, a much higher yield of the heptagon-containing isomer might be expected (at least, exceeding that of the D_{5h} isomer). However, all experimental studies in the last decade contradict this expectation. Before this work, there was only one report on the presence of the third isomer in the $\text{M}_3\text{N}@C_{2n}$ mixture. In 2006, Yang and Dunsch reported the isolation of the third isomer of $\text{Dy}_3\text{N}@C_{80}$, but its structural characterization was not possible at that time.^[12] The relative yield of $\text{Dy}_3\text{N}@C_{80}$ (III) was very low, similar to the low yield of the $\text{LaSc}_2\text{N}@C_s(\text{hept})\text{-C}_{80}$ in this work (about five times lower than that of the D_{5h} isomer).

The reason for the low yield of the $C_s(\text{hept})\text{-C}_{80}$ structures might be in the kinetic factors, that is, the ease of the structural rearrangement to other EMFs. Molecular dynamics simulations of the fullerene formation show that heptagonal rings are not uncommon for the intermediate structures, and are then annealed into the more stable fullerenes.^[13] Comparison of the $C_s(\text{hept})\text{-C}_{80}$ and $I_h\text{-C}_{80}$ isomers reveals their close similarity. These two structures are related by a Stone–Wales-like, heptagon/pentagon to hexagon/hexagon ($7/5\text{--}6/6$) realignment of the C_2 fragment (light green segment in Figure 2a,b). Our computations showed that the barrier to

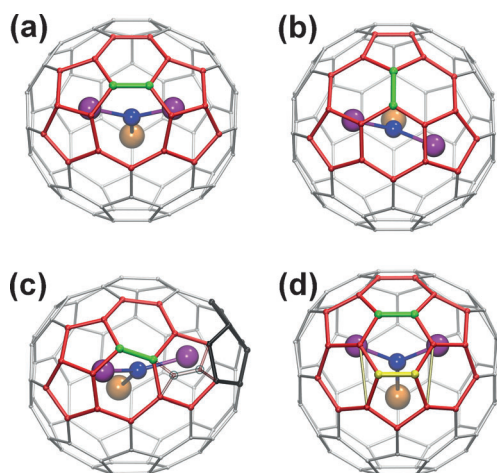


Figure 2. Molecular structures of $\text{LaSc}_2\text{N}@C_{80}$ isomers and related structures: a) $\text{LaSc}_2\text{N}@C_s(\text{hept})-C_{80}$. b) $\text{LaSc}_2\text{N}@I_h-C_{80}$. The cage fragment near the heptagon is highlighted in red, and the C–C bond which is “rotated” in the 7/5–6/6 realignment is highlighted in light green. c) $\text{LaSc}_2\text{N}@C_{78}$ with the $C_2(22010)$ cage which can be obtained from the $\text{LaSc}_2\text{N}@C_s(\text{hept})-C_{80}$ by removal of one C_2 fragment. Position of the removed fragment is shown as “ghost” atoms and the second pentagon pair in $C_2(22010)-C_{78}$ formed after removal of the C_2 fragment is highlighted in black. d) $\text{LaSc}_2\text{N}@C_{3v}(8)-C_{82}$. Removal of the C_2 fragment, highlighted in yellow, from this structure and formation of missing C–C bonds (thin yellow lines) yields the $\text{LaSc}_2\text{N}@C_s(\text{hept})-C_{80}$. Sc magenta, La orange, and N blue.

the concerted 7/5–6/6 realignment for C_{80}^{6-} is 680 kJ mol^{-1} (7.05 eV; the barrier energy is defined as the energy of the transition state. See the Supporting Information). Encapsulation of the LaSc_2N cluster reduces the barrier to 634 kJ mol^{-1} (6.57 eV). We have also tried to find if coordination of metal atoms can catalyze the 7/5–6/6 realignment. If the LaSc_2N cluster is rotated so that the Sc atom is directed towards the rearranging fragment, the barrier remains virtually the same (630 kJ mol^{-1}), whereas coordination of the La ion increases the barrier to 655 kJ mol^{-1} (6.79 eV). These values are comparable to the Stone–Wales barrier of about 7 eV as predicted at the DFT level for empty fullerenes.^[14] Encapsulation of metal atoms was also predicted to reduce the barrier. For instance, in $\text{La}@C_{60}$ the barrier is reduced to 6.26 eV (versus 7.16 in C_{60}).^[14b]

Another mechanism possibly leading to $\text{LaSc}_2\text{N}@C_s(\text{hept})-C_{80}$ and responsible for its consumption is addition/removal of a C_2 fragment.^[15] This mechanism is responsible for the formation of heptagonal rings in halogenated fullerenes.^[5a–d] Removal of the C_2 fragment from the pentagon/pentagon edge in $\text{LaSc}_2\text{N}@C_s(\text{hept})-C_{80}$ leads to $\text{LaSc}_2\text{N}@C_{78}$ with the non-IPR $C_2(22010)$ cage isomer (Figure 2c). This $\text{M}_3\text{N}@C_{78}$ isomer is usually formed in the synthesis of nitride clusterfullerenes with a large cluster size,^[16] including the $\text{LaSc}_2\text{N}@C_{2n}$ system studied in this work. In contrast, if a C_2 unit is added to the heptagonal ring of $\text{LaSc}_2\text{N}@C_s(\text{hept})-C_{80}$, the isomer of $\text{LaSc}_2\text{N}@C_{82}$ with the $C_{3v}(8)$ cage symmetry can be formed (Figure 2d). However, the $C_{3v}(8)$ cage isomer is usually the most abundant for clusterfullerenes with the formal fourfold electron transfer (e.g. carbides^[17] or sulfides),^[18] but is not common for nitride clusterfullerenes. Thus,

the formation of the $\text{LaSc}_2\text{N}@C_s(\text{hept})-C_{80}$ cage might be a result of a top-down mechanism with the transient, unstable $\text{LaSc}_2\text{N}@C_{3v}(8)-C_{82}$ as the cage precursor.^[19]

The close similarity of the $C_s(\text{hept})-C_{80}$ and I_h-C_{80} cages raises the question how the presence of the heptagonal ring affects the electronic structure of $\text{LaSc}_2\text{N}@C_{80}$. Figure 3a,b

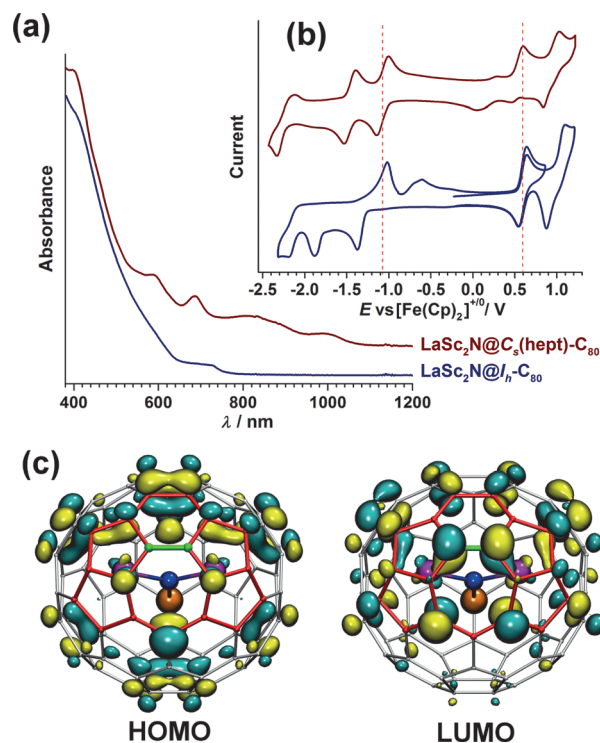


Figure 3. a) UV/Vis/NIR absorption spectra of $\text{LaSc}_2\text{N}@C_s(\text{hept})-C_{80}$ and $\text{LaSc}_2\text{N}@I_h-C_{80}$ in toluene. b) Cyclic voltammograms of $\text{LaSc}_2\text{N}@C_s(\text{hept})-C_{80}$ and $\text{LaSc}_2\text{N}@I_h-C_{80}$ in *o*-dichlorobenzene with $(n\text{Bu})_4\text{N}(\text{PF}_6)$ as a supporting electrolyte; scan rate 100 mV s^{-1} . To guide the eye, vertical dashed bars denote reduction and oxidation potentials of the $\text{LaSc}_2\text{N}@C_s(\text{hept})-C_{80}$. c) Isovalues of the HOMO and LUMO of $\text{LaSc}_2\text{N}@C_s(\text{hept})-C_{80}$ (isovalue 0.035 a.u.) computed at the PBE/TZVP level and visualized using VMD code.^[20]

compares the UV/Vis/NIR absorption spectra and cyclic voltammograms of the two isomers. Whereas the $\text{LaSc}_2\text{N}@I_h-C_{80}$ absorbs light only in the visible range (the lowest energy peak is at $\lambda = 728 \text{ nm}$, the onset is at about $\lambda = 800 \text{ nm}$), absorption of the heptagon-containing isomer is extended to the NIR range (the lowest energy peak is at $\lambda = 1000 \text{ nm}$, the onset is at about $\lambda = 1120 \text{ nm}$). Thus, the optical gap in the $C_s(\text{hept})-C_{80}$ isomer is 0.45 eV smaller and it may find use in electronic devices. Further insight into the frontier orbital energies is provided by cyclic voltammetry. Nitride clusterfullerenes usually exhibit electrochemically irreversible but chemically reversible reductions and one reversible oxidation step. $\text{LaSc}_2\text{N}@I_h-C_{80}$ is a typical example of such redox behavior (Figure 3b). In contrast, $\text{LaSc}_2\text{N}@C_s(\text{hept})-C_{80}$ exhibits two reversible reductions, but an irreversible oxidation step. The oxidation potentials of the two isomers are very similar (Table 2), near +0.6 V versus the $[\text{Fe}(\text{Cp})_2]^{+/0}$ redox couple. However, the reduction potential of the $\text{LaSc}_2\text{N}@C_s-$

Table 2: Redox potentials (V) of $\text{LaSc}_2\text{N}@C_s(\text{hept})\text{-C}_{80}$ and $\text{LaSc}_2\text{N}@I_h\text{-C}_{80}$.^[a]

$\text{LaSc}_2\text{N}@C_{80}$	gap _{EC}	Ox-II	Ox-I	Red-I	Red-II	Red-III
$C_s(\text{hept})\text{-C}_{80}$	1.69	1.04 ^[b]	0.61 ^[b]	−1.08	−1.47	−2.34 ^[b]
$I_h\text{-C}_{80}$	1.98	1.12 ^[b]	0.62	−1.36 ^[b]	−1.88 ^[b]	−2.17 ^[b]

[a] All potentials are determined by cyclic voltammetry and are referred versus $[\text{Fe}(\text{Cp})_2]^{+/0}$ redox couple. [b] Peak potentials are given for electrochemically irreversible processes

(hept)- C_{80} (−1.08 V) is substantially more positive than that in the icosahedral isomer (−1.36). Thus, the 7/5–6/6 realignment of the C_2 fragment does not affect the HOMO energy but noticeably stabilizes the LUMO.

The spatial distribution of the HOMO and LUMO in $\text{LaSc}_2\text{N}@C_s(\text{hept})\text{-C}_{80}$ is visualized in the Figure 3c. Both MOs are delocalized over the carbon cage, have noticeable but not prevailing contributions from the heptagonal ring and adjacent pentalene fragments, and have negligible contributions from the metal atoms. The LUMO has also enhanced contributions from the carbon atoms at the hexagon/heptagon edge which are highlighted in green in Figure 2 and Figure 3. Note that this bond is the shortest C–C bond in the molecule (DFT bond length 1.403 Å, the next shortest value is 1.411 Å). The crystallographic values for this C–C bond length are 1.374(15) Å and 1.362(18) Å for the two different cage orientations.

More than 25 years of the fullerene research resulted in formulation of the number of rules which govern the fullerene stability and molecular structures. One of the first rules to be established for empty cage fullerenes was the IPR, which stated that adjacent pentagons are destabilizing and should be avoided.^[2a] The avoidance of the rings other than pentagons and hexagons is another such rule which even found its way into the commonly accepted definition of fullerenes. While the IPR is a useful guide to predicting cage structures for endohedral fullerenes it was not designed for that purpose. The discovery of $\text{Sc}_3\text{N}@C_{68}$ ^[7a] and $\text{Sc}_2\text{N}@C_{66}$ ^[7b,c] in 2000 demonstrated that non-IPR cages could be stabilized when there were metals inside the cage. In this work, we showed that avoidance of heptagonal rings is also not necessary to obtain stable fullerene structures without externally attached groups. We have isolated and characterized the first endohedral metallofullerene with one heptagonal ring and proposed that its low yield may be ascribed to the kinetic factors rather than to thermodynamic stability. Hence, EMF synthesis may not be always operating under thermodynamic control.

Received: September 14, 2014

Revised: October 16, 2014

Published online: November 24, 2014

Keywords: cage compounds · density functional calculations · fullerenes · scandium · X-ray diffraction

[1] IUPAC. *Compendium of Chemical Terminology*, (the “Gold Book”), 2nd ed. (Eds.: A. D. McNaught, A. Wilkinson), Blackwell Scientific, Oxford, 2006, DOI: 10.1351/goldbook.F02547.

- [2] a) H. W. Kroto, *Nature* **1987**, 329, 529–531; b) T. G. Schmalz, W. A. Seitz, D. J. Klein, G. E. Hite, *J. Am. Chem. Soc.* **1988**, 110, 1113–1127.
- [3] a) E. Hernandez, P. Ordejón, H. Terrones, *Phys. Rev. B* **2001**, 63, 193403; b) S. Nagase, K. Kobayashi, T. Akasaka, *Theochem-J. Mol. Struct.* **1999**, 461–462, 97–104; c) P. W. Fowler, T. Heine, D. Mitchell, G. Orlandi, R. Schmidt, G. Seifert, F. Zerbetto, *J. Chem. Soc. Faraday Trans.* **1996**, 92, 2203–2210; d) A. Ayuela, P. W. Fowler, D. Mitchell, R. Schmidt, G. Seifert, F. Zerbetto, *J. Phys. Chem.* **1996**, 100, 15634–15636; e) W.-W. Wang, J.-S. Dang, J.-J. Zheng, X. Zhao, *J. Phys. Chem. C* **2012**, 116, 17288–17293; f) Z. Slanina, X. Zhao, X. Grabuleda, M. Ozawa, F. Uhlik, P. Ivanov, K. Kobayashi, S. Nagase, *J. Mol. Graphics* **2001**, 19, 252–255; g) L.-H. Gan, J.-Q. Zhao, Q. Hui, *J. Comput. Chem.* **2010**, 31, 1715–1721.
- [4] Y.-Z. Tan, S.-Y. Xie, R.-B. Huanh, I.-S. Zheng, *Nat. Chem.* **2009**, 1, 450–460.
- [5] a) P. A. Troshin, A. G. Avent, A. D. Darwish, N. Martsinovich, A. K. Abdul-Sada, J. M. Street, R. Taylor, *Science* **2005**, 309, 278–281; b) I. N. Ioffe, O. N. Mazaleva, L. N. Sidorov, S. Yang, T. Wei, E. Kemnitz, S. I. Troyanov, *Inorg. Chem.* **2013**, 52, 13821–13823; c) I. N. Ioffe, C. Chen, S. Yang, L. N. Sidorov, E. Kemnitz, S. I. Troyanov, *Angew. Chem. Int. Ed.* **2010**, 49, 4784–4787; *Angew. Chem.* **2010**, 122, 4894–4897; d) S. Yang, S. Wang, E. Kemnitz, S. I. Troyanov, *Angew. Chem. Int. Ed.* **2014**, 53, 2460–2463; *Angew. Chem.* **2014**, 126, 2492–2495; e) S. Yang, T. Wei, S. Wang, I. N. Ioffe, E. Kemnitz, S. I. Troyanov, *Chem. Asian J.* **2014**, DOI: 10.1002/asia.201402859.
- [6] Y.-Z. Tan, R.-T. Chen, Z.-J. Liao, J. Li, F. Zhu, X. Lu, S.-Y. Xie, J. Li, R.-B. Huang, L.-S. Zheng, *Nat. Commun.* **2011**, 2, 420.
- [7] a) S. Stevenson, P. W. Fowler, T. Heine, J. C. Duchamp, G. Rice, T. Glass, K. Harich, E. Hajdu, R. Bible, H. C. Dorn, *Nature* **2000**, 408, 427–428; b) C. R. Wang, T. Kai, T. Tomiyama, T. Yoshida, Y. Kobayashi, E. Nishibori, M. Takata, M. Sakata, H. Shinohara, *Nature* **2000**, 408, 426–427; c) M. Yamada, H. Kurihara, M. Suzuki, J. D. Guo, M. Waelchli, M. M. Olmstead, A. L. Balch, S. Nagase, Y. Maeda, T. Hasegawa, X. Lu, T. Akasaka, *J. Am. Chem. Soc.* **2014**, 136, 7611–7614; d) A. A. Popov, S. Yang, L. Dunsch, *Chem. Rev.* **2013**, 113, 5989–6113; e) B. Q. Mercado, C. M. Beavers, M. M. Olmstead, M. N. Chaur, K. Walker, B. C. Holloway, L. Echegoyen, A. L. Balch, *J. Am. Chem. Soc.* **2008**, 130, 7854–7855.
- [8] S. Stevenson, C. B. Rose, J. S. Maslenikova, J. R. Villarreal, M. A. Mackey, B. Q. Mercado, K. Chen, M. M. Olmstead, A. L. Balch, *Inorg. Chem.* **2012**, 51, 13096–13102.
- [9] a) L. Dunsch, S. Yang, *Small* **2007**, 3, 1298–1320; b) S. F. Yang, L. Dunsch, *J. Phys. Chem. B* **2005**, 109, 12320–12328; c) J. Zhang, S. Stevenson, H. C. Dorn, *Acc. Chem. Res.* **2013**, 46, 1548–1557.
- [10] a) A. A. Popov, L. Dunsch, *J. Am. Chem. Soc.* **2007**, 129, 11835–11849; b) A. Rodríguez-Fortea, N. Alegret, A. L. Balch, J. M. Poblet, *Nat. Chem.* **2010**, 2, 955–961.
- [11] D. N. Laikov, Y. A. Ustynuk, *Russ. Chem. Bull.* **2005**, 54, 820–826.
- [12] S. F. Yang, L. Dunsch, *Chem. Eur. J.* **2006**, 12, 413–419.
- [13] S. Irle, G. S. Zheng, M. Elstner, K. Morokuma, *Nano Lett.* **2003**, 3, 1657–1664.
- [14] a) H. F. Bettinger, B. I. Yakobson, G. E. Scuseria, *J. Am. Chem. Soc.* **2003**, 125, 5572–5580; b) W. I. Choi, G. Kim, S. Han, J. Ihm, *Phys. Rev. B* **2006**, 73, 4.
- [15] P. W. Dunk, N. K. Kaiser, C. L. Hendrickson, J. P. Quinn, C. P. Ewels, Y. Nakanishi, Y. Sasaki, H. Shinohara, A. G. Marshall, H. W. Kroto, *Nat. Commun.* **2012**, 3, 855.
- [16] a) A. A. Popov, M. Krause, S. F. Yang, J. Wong, L. Dunsch, *J. Phys. Chem. B* **2007**, 111, 3363–3369; b) C. M. Beavers, M. N. Chaur, M. M. Olmstead, L. Echegoyen, A. L. Balch, *J. Am. Chem. Soc.* **2009**, 131, 11519–11524; c) A. L. Svitova, A. A.

- Popov, L. Dunsch, *Inorg. Chem.* **2013**, 52, 3368–3380; d) J. Zhang, D. W. Bearden, T. Fuhrer, L. Xu, W. Fu, T. Zuo, H. C. Dorn, *J. Am. Chem. Soc.* **2013**, 135, 3351–3354.
- [17] Y. Iiduka, T. Wakahara, K. Nakajima, T. Tsuchiya, T. Nakahodo, Y. Maeda, T. Akasaka, N. Mizorogi, S. Nagase, *Chem. Commun.* **2006**, 2057–2059.
- [18] L. Dunsch, S. Yang, L. Zhang, A. Svitova, S. Oswald, A. A. Popov, *J. Am. Chem. Soc.* **2010**, 132, 5413–5421.
- [19] J. Zhang, F. L. Bowles, D. W. Bearden, W. K. Ray, T. Fuhrer, Y. Ye, C. Dixon, K. Harich, R. F. Helm, M. M. Olmstead, A. L. Balch, H. C. Dorn, *Nat. Chem.* **2013**, 5, 880–885.
- [20] W. Humphrey, A. Dalke, K. Schulten, *J. Mol. Graphics* **1996**, 14, 33–38.
-